Simultaneous scanning tunneling microscopy and stress measurements to elucidate the origins of surface forces

Tetsuya Narushima,[a)] Niall T. Kinahan,[b)] and John J. Boland[c)]
School of Chemistry, Trinity College Dublin, Dublin 2, Ireland and The Centre for Research on Adaptive Nanostructures and Nanodevices (CRANN), Trinity College Dublin, Dublin 2, Ireland

(Received 21 July 2006; accepted 9 April 2007; published online 11 May 2007)

We have developed a new combined measurement system to investigate the underlying origins of forces on solid state surfaces from the viewpoint of atomic surface morphology. This system consists of two main parts: the measurements of force based on displacements and detailed atomic resolution observations of the surface morphology. The former involves a large sample cantilever and a capacitive detection method that provide sufficient resolution to detect changes of a few meV/atom or pN/atom at surfaces. For the latter, a scanning tunneling microscope was incorporated to observe structural changes occurring on the surface of the cantilever sample. Although this combined observation is not trivial, it was accomplished by carefully designing sample dimensions while suppressing the self-oscillation of the cantilever. To demonstrate the performance of this system a preliminary study of the room temperature adsorption of Br_2 on the clean Si(111)-7×7 surface is presented. © *2007 American Institute of Physics.* [DOI: 10.1063/1.2736417]

INTRODUCTION

Feynman said that "many of the problems of molecular structure are concerned essentially with forces."[1] This assertion is also valid for atomic scale structures and phenomena on surfaces. For example, in the case of nonmetallic samples, when a new surface is created, the excess energy due to unsaturated dangling bonds at the surface can be lowered by forming additional bonds. The creation of these additional bonds involves atomic displacements which result in surface *strain*.[2–4] As a result of the competition between energy lowering by the creation of additional bonds and the energy increase due to strain, superstructures on the surface can be identified each with its own *intrinsic surface stress*. In the case of adsorbates on surfaces, an adsorbate-induced surface stress occurs due to redistribution of surface charge, atomic size differences, bond angle and distance changes, and the stiffness of these bond lengths and angles with regard to distortions. For ultrathin film growth, surface and *interface stresses* play an important role in determining the subsequent growth mode.[5,6] The presence of these forces on surfaces are seldom considered largely because both the atomic scale surface structure and reaction phenomena can often be successfully explained without considering stress. However, as structural scales become increasingly smaller, the role of these forces cannot be ignored.[7–13]

Several methods have already been developed to determine the effects of such forces at surfaces. Some are based on measurements of lattice distortion such as the use of x-ray diffraction (XRD), electron beam diffraction [low-energy electron diffraction (LEED) and reflection high-energy electron diffraction (RHEED)], infrared spectroscopy [Fourier transform infrared (FTIR)], and Raman spectroscopy [surface-enhanced Raman scattering (SERS)]. The others are based on measurements of sample bending. The former enables us to detect only the periodicity of ordered structures and/or local information regarding sample distortion. Sample bending, on the other hand, captures and integrates the effects of all such forces. In fact, the measurements of sample bending has led to the discovery of new methods and phenomena, for example, defect counting and athermal stress relaxation,[12,13] which would never have been identified via measurements of the lattice distortion. This clearly indicates that the measurement of surface forces has the potential to provide fundamental insights into surface structure and adsorption phenomena.

In reality, however, it is difficult to discuss the atomic scale origins of new stress phenomena using only the measurements of sample bending. For this reason, some other complementary methods should be available. To investigate the origin surface stress from the viewpoint of *atomic surface morphology*, a direct observation of the structure is necessary. Previously, surface stress measurements based on the sample bending were separately combined with independent scanning tunneling microscopy (STM) studies and were found to be extremely useful in revealing the underlying atomic scale origins of the measured surface stress.[12–14] To realize a simultaneous capability to measure both stress and STM we have developed a measurement system in which STM is performed on the same cantilever sample used for measuring the sample bending. This system enables us to directly and visually explore the origins of such forces, providing us with structural, dynamical, and interactional information which will prove to be extremely useful in understanding and improving atomic scale phenomena. In this

[a)]Present address: Institute for Molecular Science, National Institutes of Natural Sciences, 38 Nishigo-Naka, Myodaiji, Okazaki 444–8585, Japan; electronic mail: naru@ims.ac.jp
[b)]Electronic mail: kinahan@tcd.ie
[c)]Electronic mail: jboland@tcd.ie

 © 2007 American Institute of Physics

Downloaded 26 Sep 2007 to 133.48.150.181. Redistribution subject to AIP license or copyright, see http://rsi.aip.org/rsi/copyright.jsp

article, we describe the actual experimental setup and also demonstrate the performance and capability of this system.

EXPERIMENT

A cantilever sample is the simplest structure available to measure sample bending. This bending is induced by forces acting at the surface region. However, to achieve atomic scale resolution via STM on the cantilever used to measure stress, we are faced with several significant challenges.

One such challenge concerns the stability of STM observation on the cantilever sample. A conventional STM sample is clamped at both ends. Consequently, highly resolved STM imaging can be performed, displaying atomic features. However, oscillation of the cantilever sample due to its structural design, i.e., natural resonance, affects the quality of the observation. In general, a simple solution to suppress this oscillation is to use a thick sample. On the other hand, to measure sample bending, a thinner sample is more preferable. It is therefore imperative to carefully choose the dimensions of the cantilever sample for a simultaneous measurement.

Another major challenge relates to sample heating. Most sample heating methods are based on the premise that both ends of the sample are clamped. Silicon surfaces, for example, are predominantly heated using both ends of the sample as electrodes and allowing a current to be passed through the sample. However, this type of direct heating method is not available for a cantilever sample. To overcome this, we adopt two heating methods depending on when heating was required *before* or *during* measurements. For sample heating before measurements, i.e., sample preparation including surface cleaning and annealing, a method using bimetallic strips was developed.[15] The bimetallic strips are used to make electrical contacts allow current to pass through a defined region of the sample. With this method, we can control temperatures of the sample up to approximately 1400 K. For sample heating during measurements, it is critical to have no physical contact with the sample, and, as a result, some indirect heating method is required. Consequently, we use an infrared indirect heating method that allows us to statically heat up the sample to approximately 950 K.

Sample bending detection

When a sample surface undergoes any type of reaction or surafce modification, the sample bends due to forces induced by this process and is detected via deflection of the cantilever sample. From this deflection, the forces acting in the surface region can be estimated. The deflections are typically not large, and in the case of atomic scale forces the deflection is typically on the order of nanometers. In order to measure minute deflections, and hence to have greater force resolution, we have to carefully consider a method to detect this sample bending.

Several methods are available to detect the deflection of the cantilever sample. *Optical techniques* include an optical cantilever bending method,[11–13] similar to that used in an atomic force microscopy[16] (AFM) and interferometery.[17] With regard to *electrical techniques*, STM (Refs. 9 and 18) and capacitance[9] methods are also available.

Each method has advantages and disadvantages. The optical cantilever bending method has a good detection limit (typically about 2×10^{-4} N/m in total stress change) and is well established. However, this method is preferable for small micron scale cantilevers because the change of angle at the free end is detected to quantify sample deflection. On the other hand, the electrical techniques mentioned above are more practical for large cantilevers, as the change of position at the free end is detected to measure the deflection. This is also advantageous as it frees us from the awkwardness of fabricating small cantilever samples. Nonetheless, such electrical techniques are not easily measured in strong electric and magnetic fields or in charged environments such as plasmas and ionic solutions. The STM method[13] can detect cantilever deflections and observe atomic structures simultaneously. However, with this method it is difficult to obtain a similar detection limit to that of the optical cantilever bending method because, in principle, thermal drift and/or the unknown shape of the STM tip induces uncertainty in measurements. Typically, this method achieves a resolution of approximately 1×10^{-1}–1×10^{-2} N/m in total stress change.[13] In contrast, the capacitance method which uses a well defined reference electrode, unlike the STM method, has a superior detection limit of $\pm6.9\times10^{-3}$ N/m in total stress change.[19] This stress value corresponds to an energy change of approximately 1–10 meV/atom at the surface. In order to achieve a good detection limit with the use of large cantilever samples, we adopted the capacitance system of Sander and Ibach[19] to quantify sample bending.

Visualization via STM

In order to observe surface structures on a cantilever surface that is measuring sample bending, movements of the cantilever must be recognized and managed. During surface modification, two types of movement are important—one due to the natural oscillation of the cantilever sample itself and the other induced by forces acting in the surface region.

To detect sample deflection, it is beneficial to use a cantilever sample which is as long and thin as possible since surface modifications will result in larger displacements at the free end. However, difficulty arises regarding structural observations with this setup due to the natural oscillation of the cantilever sample itself. Without suppressing this inherent movement, atomic structural observation may not be possible. Thus, it is necessary to minimize movement due to natural resonance via tailoring of the cantilever dimensions.

The deflection density, $\sqrt{(\partial/\partial f)(\delta z)^2}|_{f=f_0}$, of the cantilever sample at the oscillation peak can be obtained from the following expression: $\sqrt{(\partial/\partial f)(\delta z)^2}|_{f=f_0}=\sqrt{2k_BTQ/\pi kf}$, where δz, f, f_0, T, k, k_B, and Q represent the displacement of the cantilever sample at the free end, the frequency of the self-oscillation, the peak frequency of the self-oscillation, the temperature, the spring constant, the Boltzmann constant, and the quality factor of the cantilever sample, respectively.[20] Assuming a Gaussian distribution at $f=f_0$ and by using the definition of the quality factor, $Q\equiv f_0/\Delta f$, we can approxi-

Downloaded 26 Sep 2007 to 133.48.150.181. Redistribution subject to AIP license or copyright, see http://rsi.aip.org/rsi/copyright.jsp

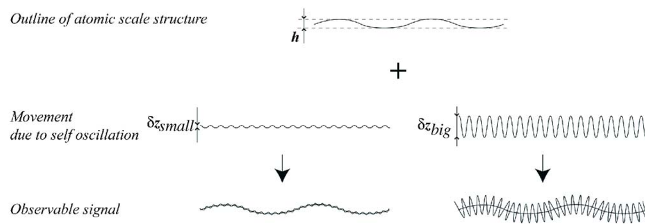

FIG. 1. Schematic diagram representing the observable STM topographical signal for a cantilever sample. The signal consists of a mixture of the outline of the atomic structure to be observed and movement induced by the self-oscillation. If the movement is sufficiently small, the original atomic scale structure can be rebuilt from the signal by use of a fast Fourier transformation (FFT) filter.

mate the root mean square of the displacement, $\delta z_{\rm rms} \approx \sqrt{2k_B TQ/\pi k f}\sqrt{f_0/Q} = \sqrt{2k_B T/\pi k}$. This estimation provides us with valuable information concerning the deflection induced by the self-oscillation. In reality, the peak-to-peak amplitude, $\delta z_{\rm p\text{-}p} = 2\sqrt{2}\,\delta z_{\rm rms} \approx 4\sqrt{k_B T/\pi k}$, should be calculated to quantify the actual displacement at the free end. From $\delta z_{\rm p\text{-}p}$, it is found that the spring constant and the temperature dictate the movement. Therefore, $\delta z_{\rm p\text{-}p}$ is proportional to $(t/l)^{-3/2} w^{-1/2}$ at constant temperature since the spring constant $k = Ewt^3/4l^3$, where w, t, l, and E are width, thickness, length, and Young's modulus of the cantilever sample, respectively. This implies that if w, and l are known, we can suppress the movement due to the self-oscillation by choosing an appropriate value of t, thus allowing atomic scale structures to be observed.

In general, however, the observed STM topographical signal for a cantilever sample contains both atomic scale structure and self-oscillation features. As both features are independent, i.e., with no energetic interaction, this can be described with a simple topographical summation in real space, as shown in Fig. 1. In Fig. 1, we assume two self-oscillation conditions, $\delta z_{\rm small}$ and $\delta z_{\rm big}$, where $\delta z_{\rm small} < h < \delta z_{\rm big}$, with h as the height of the atomic scale structure. As a result, the observable STM topographical signal is constantly modified by the natural movement. Consequently, to acquire highly resolved STM images, we have to suppress $\delta z_{\rm p\text{-}p}$.

Figure 2 displays the expected displacement at the free end, $\delta z_{\rm p\text{-}p}$, of a Si(111) cantilever sample induced by self-oscillation. Here, the dimensions of the sample are assumed to be 50 mm long and 10 mm wide so as to mimic the cantilever sample used by Sander and Ibach.[19] The well-known Si(111)-7×7 reconstruction is a nice example to test the performance of our system. The step height of the surface is 0.5 nm. The basis vector length is 2.69 nm and the height of an adatom protrusion is approximately 50 pm. To resolve these adatoms on the Si(111)-7×7 surface, it is required that $\delta z_{\rm p\text{-}p}$ be smaller than the 50 pm protrusions. For this condition we estimated the critical thickness of the cantilever to be 0.13 mm (k=8.4 N/m). In the case of a 0.1 mm thick cantilever sample (k=3.7 N/m), the estimated value for $\delta z_{\rm p\text{-}p}$ is 75 pm. Since this circumstance corresponds to $\delta z_{\rm big}$ in Fig. 1, it would prove difficult to resolve the adatoms on the Si(111)-7×7 surface. To resolve these adatoms sufficiently, $\delta z_{\rm p\text{-}p}$ should be approximately ten times smaller than the protrusions, thus representing $\delta z_{\rm small}$ in Fig. 1. This condition corresponds to a thickness of approximately 0.5 mm. For example, a 6.25 pm displacement at the free end can be estimated for a 0.525 mm thick cantilever sample (k=539.7 N/m). Therefore, we can expect to resolve the adatoms on the Si(111) surface using a cantilever sample that is thicker than 0.525 mm.

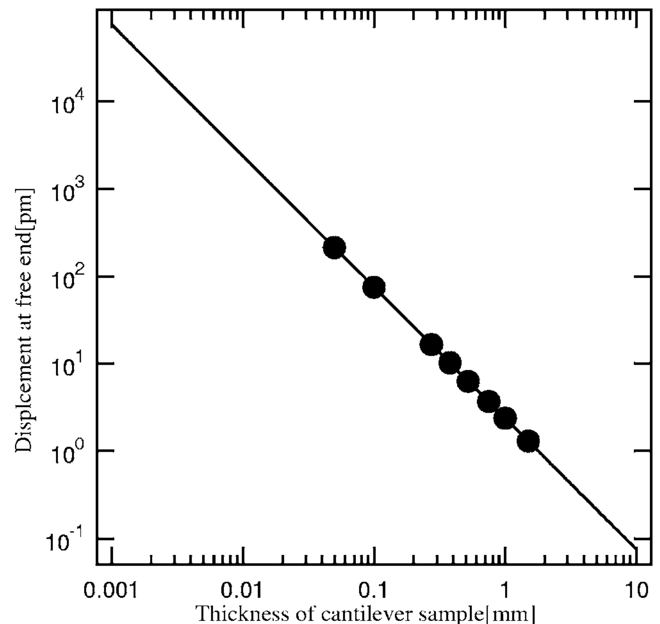

FIG. 2. Expected displacement at the free end, $\delta z_{\rm p\text{-}p}$, of a Si(111) cantilever sample induced by self-oscillation as a function of thickness. Dimensions of the sample: 50 mm long and 10 mm wide. Each dot represents thicknesses of 0.05, 0.10, 0.275, 0.380, 0.525, 0.750, 1.00, and 1.50 mm.

Thus far, displacements at the free end of the cantilever were discussed in relation to the STM observation. However, for our system, it is preferable to use the free end region of the sample to detect sample bending, as displacements are greater at this point. As a result we chose the center of the cantilever for surface modification and structural observation via STM. STM at this region has the added advantage of reducing the estimated value of $\delta z_{\rm p\text{-}p}$ by half, resulting in improved STM resolution.

Design concepts

Our system is intended to simultaneously measure sample bending and observe surface structure via STM. To realize this, the design of the sample holder is critical for an accurate performance. Figure 3 presents a schematic of our system. The component to detect sample bending includes a cantilever sample, a reference electrode, and a clamping base. The additional component consists of a STM which images the central area on the cantilever sample which is accessible to reaction and surface modification.

Sample deflection can be measured by monitoring the change of capacitance between the cantilever sample and the reference electrode. From the measured capacitance value, the displacement at the free end of the cantilever sample can be calculated, allowing the actual deflection to be estimated. A structural observation on the cantilever sample via STM

Downloaded 26 Sep 2007 to 133.48.150.181. Redistribution subject to AIP license or copyright, see http://rsi.aip.org/rsi/copyright.jsp

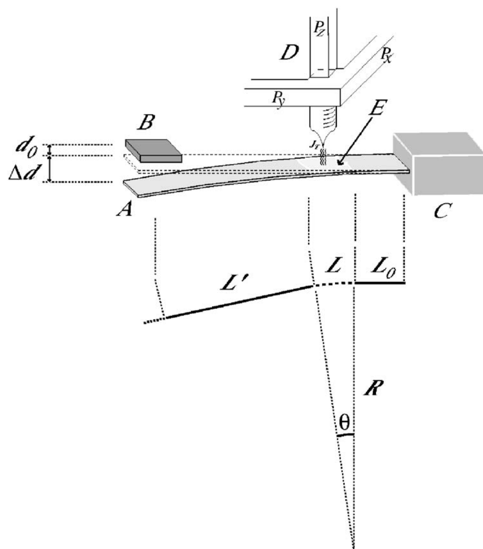

FIG. 3. System for the measurement of sample bending and structural observation. The detection component for sample bending consists of a cantilever sample (A), a reference electrode (B), and a clamping base (C). The additional component for structural observation consists of a cantilever sample (A) and a STM (D), which observes the effective modification area (E). Sample bending is induced by atomic scale modifications which occur only in region E.

can be performed before, during, or after such measurements.

Figure 4 represents a three-dimensional computer aided design (CAD) system image of our actual cantilever sample holder. A cantilever sample with dimensions $50 \times 10 \times 0.525$ mm^3 is used. To form the cantilever structure, we first prepare a rectangular shaped sample with dimensions $60 \times 10 \times 0.525$ mm^3. Following this, one end is fixed in the clamping base, i.e., the $10 \times 10 \times 0.525$ mm^3 region. Uniform modification of the cantilever sample is necessary for measurement and interpretation of forces acting at

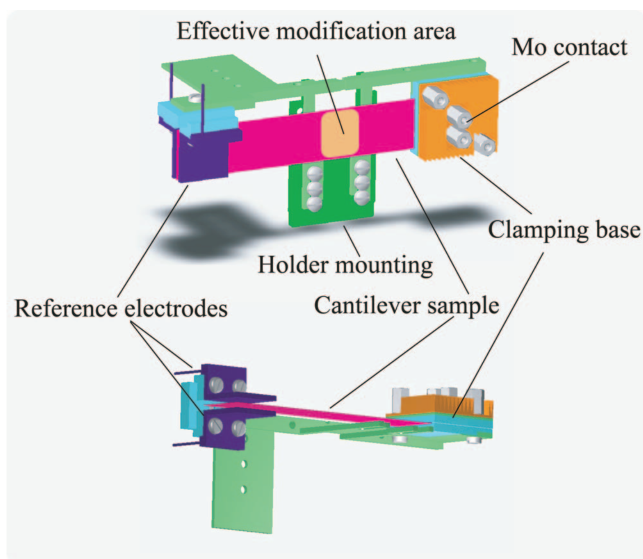

FIG. 4. (Color) A three-dimensional CAD image of our actual cantilever sample holder. Each color represents different materials: green, light blue, navy blue, orange, and pink correspond to super invar, quartz, cupper, and silicon, respectively.

the surface region. However, uniform reaction or modification of a 50×10 mm^2 surface area would prove to be extremely difficult. Therefore, the center 10×10 mm^2 area was chosen to meet this criterion. Passivation of the silicon sample is achieved with the use of a native oxide layer which covers the entire surface region. However, in order to create a clean 10×10 mm^2 Si surface, which acts as the effective modification area, regionalized heating is required.[15] The heating method used will be discussed in a subsequent section. The center of this area is located 15 mm from the fixed end of the cantilever sample.

Most components of the sample holder are made from super invar because it has a very low thermal expansion coefficient. This material is therefore suitable for stable STM and sample bending measurements, showing only small instabilities due to high temperature effects and/or temperature fluctuations. Quartz is also known to have a low thermal expansion coefficient. For that reason, super invar and quartz are used for the conducting and insulating parts, respectively. This combination has an added advantage for the clamping component of the sample holder. Here, not only is the use of low thermal expansion materials important in minimizing undesired effects, but matching these thermal expansion coefficients is equally important to avoid interface stress as in a bimetallic strip.[15] In fact, super invar and quartz have thermal expansion coefficients of 0.4×10^{-6} and 0.5×10^{-6} °C^{-1}, respectively. The clamping base (including the fixed end) was formed with a sandwich structure of quartz and super invar, i.e., super invar—quartz—silicon—quartz—super invar. However, to apply electric potential to the silicon sample for STM, a plate spring contact made from molybdenum is employed. Mo prevents metal contamination of the sandwich structure. In addition, a copper heat sink is added to one side of this sandwich structure to radiate away excess heat and therefore allow thermal equilibrium to be quickly established.

At the free end, two reference electrodes are set to detect the capacitance values between the sample and each reference electrode. We assume that this configuration forms a simple parallel plate capacitor. Each electrode is supported by a quartz base. Ordinarily, one of the electrodes is required to measure the displacement, while the other acts as a credibility test for the measured displacement. The distance between these two electrodes is 2 mm. The cantilever sample is located in between these electrodes, and thus the distance between the cantilever sample and each electrode is less than 1 mm. Each electrode has a 10×10 mm^2 surface area, and the exact center position of the electrode is situated 45 mm from the fixed end. Both electrodes are made from molybdenum to prevent metal contamination of the sample in the event of contact. Furthermore, to avoid measurement of a parasitic capacitance due to the nature of the semiconducting sample, an electrical bypass electrode is attached to the silicon. The bypass permits a bias to be applied to the free end of the sample only. This shortcut consists of a flexible metallic wire that is directly connected to a 10×10 mm^2 Ta foil which tightly encapsulates the free end region of the sample. The Ta foil does not contaminate the sample.

Figure 5 displays a photograph of our system. Using the

Downloaded 26 Sep 2007 to 133.48.150.181. Redistribution subject to AIP license or copyright, see http://rsi.aip.org/rsi/copyright.jsp

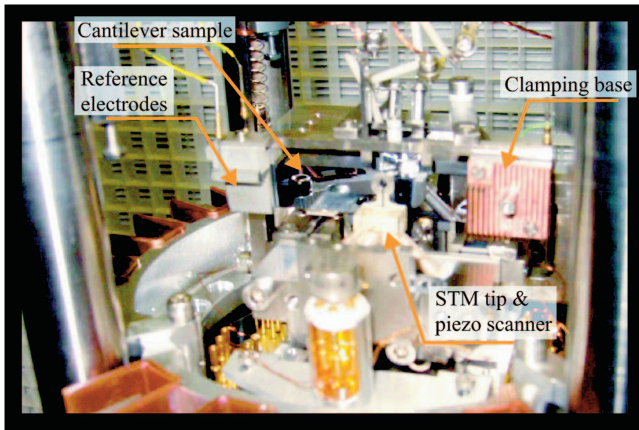

FIG. 5. (Color) Photograph of our developed system. This system consists of a cantilever sample holder designed by us and an Omicron UHV STM-1 (Ref. 21).

sample holder mounting displayed in Fig. 4 allows the setup to be fitted to a conventional STM unit. We chose a room temperature STM, namely, the Omicron ultrahigh vacuum (UHV) STM-1.[21] The imaging of a surface requires mechanical stability of the tip, the sample, and their holders. Mechanical isolation from the external environment is also critical. Conventional STM systems are well established with regard to these requirements. Specifically, the STM-1 has a special spring suspension system with eddy current damping, which ensures excellent vibration isolation (resonance frequency is <2 Hz). Such isolation is preferable not only for STM observation but also for sample bending detection. With regard to the STM-1 system, the tip is mounted tightly on a tripod scanner, which consists of a triple tube arrangement that is fixed to the STM stage. However, due to the architecture of our required sample holder, the region to be scanned is located 9 mm above the original conventional STM location. To compensate for this height difference, the position of the STM scanner was raised using a 2 mm thick stainless steel plate.

A sample pusher

In addition to the above, our system is also equipped with a device for sample *pushing*. This device can be used for applying external stress to the sample mechanically, although this will not be discussed in this article. To push the sample, a microslide piezo, Omicron MS5,[21] is used. This slider can provide 40 nm step displacements of the cantilever sample at a minimum, while the resultant displacements can be detected by the capacitance change.

Determination of sample bending

As previously mentioned, sample bending can be detected capacitively. Here, we will discuss a conversion method from capacitance values to deflections and forces. Initially, a pair of parallel plates which have a spacing d_0 and equivalent surface areas S under UHV conditions result in a capacitance value, $C(d_0)=\varepsilon_0 S/d_0$. When there is a spacing variation from d_0, namely, Δd, the change in capacitance is given by

$$\Delta C(\Delta d) \equiv C(d_0+\Delta d) - C(d_0) \cong \frac{\varepsilon_0 S}{d_0^2}\Delta d, \tag{1}$$

where ε_0 is the dielectric constant for a vacuum and assuming $\Delta d \ll d_0$. Figure 3 displays a small displacement at the free end, Δd, from the initial spacing d_0. Along the longitudinal direction of the cantilever, the lever part can be divided into three regions, L_0, L, and L'. The effective modification area, i.e., region L, is located between the fixed end region, L_0, and free end region, L'. It should be noted that the L' region terminates at the center of the reference electrode, as displayed in Fig. 3. Hence, the small displacement at the free end originates only from region L, while regions L_0 and L' do not display any deflection.

To quantify the deflection by means of the displacement Δd, it is necessary to establish the radius of curvature R, for region L. Let L and l represent the arc and its chord, respectively, of the circle segment with central angle θ and radius R.

Subsequently, the displacement is given by

$$\Delta d = l \sin\frac{\theta}{2} + L' \sin\theta \cong \left(\frac{L^2}{2} + LL'\right)\frac{1}{R}, \tag{2}$$

The above approximation is valid, assuming that $l \cong L$, which is true when $\theta \ll \pi/2$.

In order to estimate the forces contributing to the sample bending, we use the Stoney-Hoffman equation[22,23]

$$h \cdot \sigma = \frac{Et^2}{6(1-\nu)}\frac{1}{R}, \tag{3}$$

where ν, σ, and h represent Poisson's ratio, the force per unit area along the longitudinal direction of the cantilever, and the effective thickness of the atomically strained layer, respectively. Finally, utilizing Eqs. (1)–(3), we obtain an equation converting the capacitance change to force change induced at the surface region,

$$h \cdot \sigma(\Delta d) = \frac{t^2}{6}\left\{\frac{1}{L^2/2 + LL'}\right\}\frac{E}{(1-\nu)}\frac{\varepsilon_0 S}{C(d_0)^2}\Delta C(\Delta d). \tag{4}$$

From Eq. (4), it is evident that in order to have the capability to detect atomic scale forces, a precise means of sensing capacitance changes is vital. To achieve this we use an Andeen-Hagerling AH 2550A (Ref. 24) capacitance bridge. The AH 2550A enables us to detect extremely small changes in the capacitance value, between 0.5–0.8 aF. With this detection resolution and considering our system, i.e., $t=525\times10^{-6}$ m, $L=1.0\times10^{-2}$ m, $L'=2.5\times10^{-2}$ m, $S=10^{-4}$ m^2, $\varepsilon_0=8.854\times10^{-12}$ C^2/N m^2, and $E/(1-\nu)|_{\mathrm{Si}(111)}=2.29\times10^{11}$ N/m,[25] the theoretical detection limit for the displacement at the free end of the cantilever sample and the force induced are estimated to be 0.71 Å and 2.48×10^{-3} N/m, respectively. In estimating these values we used a value of $C(d_0)=3.0$ pF as an initial capacitance value [this $C(d_0)$ value typically varies between 2.5 and 3.5 pF depending on the clamping condition]. In reality, our capacitance resolution, including noise, is reduced slightly, i.e., ±1.9 aF, which will be statistically deduced later, giving values of ±1.87 Å and $\pm6.55\times10^{-3}$ N/m for the displacement and force detection

Downloaded 26 Sep 2007 to 133.48.150.181. Redistribution subject to AIP license or copyright, see http://rsi.aip.org/rsi/copyright.jsp

limits, respectively. Assuming an effective thickness for the strained layer of $h=0.1$ or 0.5 nm provides us with a strain energy detection limit of ±8.2 or ±1.6 meV/atom, when all force in the effective modification area is assigned to surface strain. It is important to note that these values are much smaller than those associated with bonding energies. In addition, sample bending is basically caused by lateral force. In the case of Si(111), the force per atom detection limit along the $[1\bar{1}0]$ direction corresponds to ±6.82 or ±1.37 pN/atom for $h=0.1$ or 0.5 nm, respectively. This is almost comparable with the force detection limit in noncontact atomic force microscopy (nc-AFM). Hence, our system is adequate to study the origins of forces in atomic scale structures and phenomena on surfaces.

Heating a cantilever sample: Direct and indirect methods

To heat up our cantilever sample, we used two varieties of sample heating methods, i.e., direct and indirect means. For sample preparation including surface cleaning and annealing before measurements, typically very high temperature regionalized heating is required. At this stage, physical contact with the cantilever sample is permitted. To achieve this, we developed special controllable contacts formed using bimetallic strips.[15] The bimetallic strips are heated using a filament, causing them to deflect towards the cantilever sample. Physical contacts with the sample are made under appropriate conditions. A current can then be passed through the cantilever sample using these contact points. Using this technique, a 10×10 mm^2 region of the sample can be heated up by placing two bimetallic strips at the back side of the effective modification area of the cantilever sample with a 10 mm spacing between them. In the case of a Si cantilever sample, it is possible to flash the sample with the above-mentioned method. Following the flash, all contacts between the sample and strips are broken as desired. Details of this method are explained elsewhere.[15]

On the other hand, for the duration of measurements, any physical contact with the cantilever sample is totally forbidden. Therefore, only indirect heating methods are acceptable. There are typically two methods available—electron bombardment and radiative heating.[26] For our system, the former method may affect the reliability of measured capacitance values due to the strong electric field required to accelerate electrons. In contrast, the latter method can be electrically static. To employ this method the radiation has to be directed solely towards the cantilever sample surface in order to heat up the effective modification area effectively and to conduct UHV experiments. For our system, we chose an infrared heating system with a quartz light guide.[27] This system basically consists of a high power 3 kW infrared light bulb with a 900 nm peak intensity, an aurous elliptically shaped focusing mirror, and a quartz light guide. Using a sapphire viewing port, the infrared light is directed towards the effective modification area of the cantilever sample by total internal reflection through the light guide.

However, due to space limitations in the vicinity of the STM and the cantilever sample holder (shown in Fig. 6), measures had to be taken to appropriately direct light towards the sample surface. To overcome this we utilized refraction effects due to a sharp end. The sharp end has an off cut 30° from its cross section, and the light guide stands at a 20° offset angle from the vertical direction. This setup provides us with an 8×10.4 mm^2 heating area at the effective modification region. With this method we can achieve temperatures up to approximately 950 K.

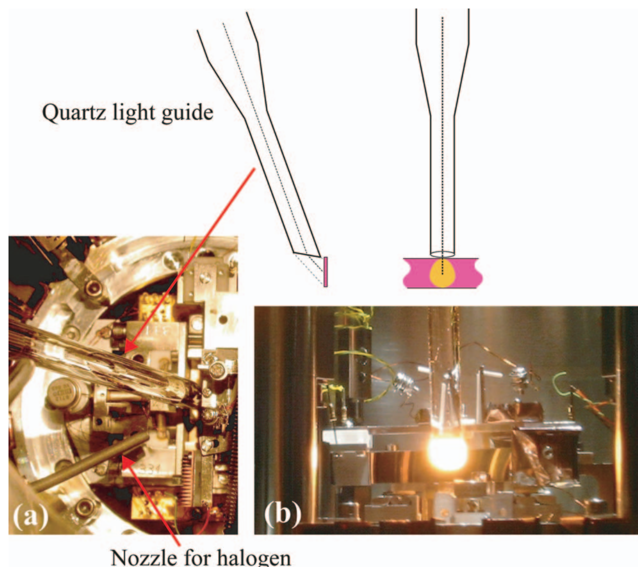

FIG. 6. (Color) Setup for the infrared heating system. Pictures (a) and (b) display views both from above and from the front side of the cantilever sample holder, respectively. To introduce infrared light into the system via the infrared light bulb, a quartz light guide was used. The wide and narrow parts of the light guide have 20.6 and 8 mm diameters, respectively. The sharp end has an off cut 30° from its cross section and the light guide stands at a 20° offset angle from the vertical direction. By use of refraction through the sharp end, the infrared light can be directed towards the effective modification area of the cantilever sample surface.

PERFORMANCE

STM imaging on the cantilever sample

In order to discuss the quality of the STM imaging on the cantilever sample, let us observe a clean Si(111)-7×7 reconstructed surface. The clean Si(111)-7×7 surface was made using the bimetallic strip heating method.[15] During sample cleaning, the base pressure in the UHV chamber was lower than 1.3×10^{-10} Torr. The Si(111) cantilever sample used was cut from a single-side mirror polished 5 in. wafer which was *p*-type boron doped, with a thickness of 525 ± 10 μm and a resistivity of 5.0–18.0 Ω cm. The wafers were supplied by Shin-Etsu Chemical Co., Ltd. Figure 7 displays a typical STM image of a Si(111)-7×7 surface observed on the cantilever sample using our setup. The image quality has been significantly improved since our previous report.[15] From the image, each adatom is clearly resolved and some reacted sites can be easily recognized.

However, there is approximately ±4 pm noise fluctuations in the image cross section along the same line scan, shown as a green dashed line in Fig. 7. The noise source may be due to induced electrical effects and/or the STM tip. Another possible source is the natural oscillation of the cantile-

Downloaded 26 Sep 2007 to 133.48.150.181. Redistribution subject to AIP license or copyright, see http://rsi.aip.org/rsi/copyright.jsp

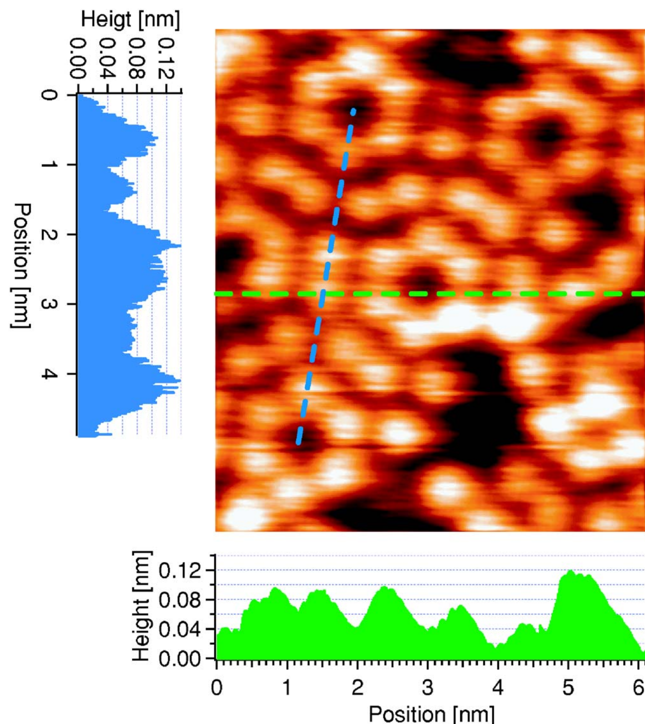

FIG. 7. (Color online) A typical STM image of the Si(111)-7×7 surface taken on the cantilever sample. This image was taken with a sample bias of +0.7 V and a tunneling current of 0.01 nA. The image size is 6.2×7.2 nm^2. This image was scanned from left to right. The green and blue dashed lines represent cross sections along similar and different scan lines.

ver sample itself. In contrast, a different scan line, shown as a blue dashed line in Fig. 7, displays ±7.5 pm noise fluctuations.

Nonetheless, although there are ways to improve the quality of the imaging technique, at present it is sufficient to observe and discuss atomic scale structures and phenomena for the immediate future.

Detection limit for capacitance measurement and its stability

In order to discuss the forces acting at the surface region, not only are precise capacitance measurements essential, but mechanical, electrical, and thermal stabilities also play pivotal roles. Figure 8 displays a typical time evolution of the capacitance change. Analysis indicates that we have very little thermal drift, approximately -0.39×10^{-7} pF/s.

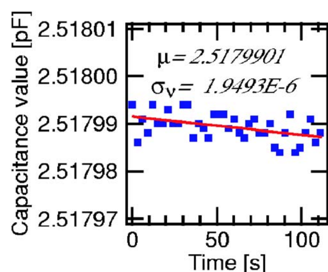

FIG. 8. (Color online) Time evolution of the capacitance change. The red solid line was drawn using linear curve fitting and represents a tiny slope due to thermal drift.

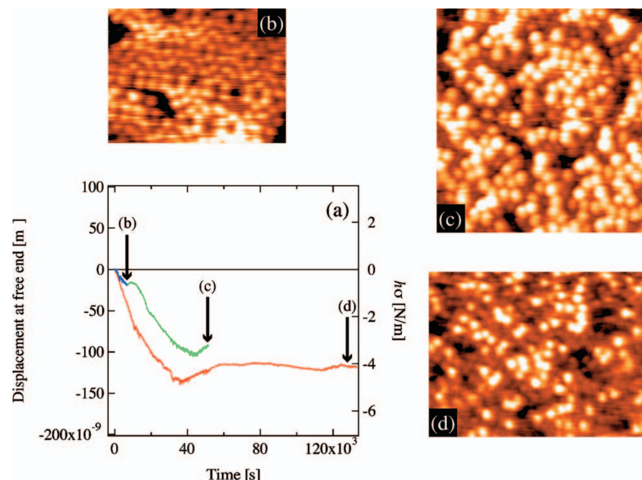

FIG. 9. (Color) Example of a simultaneous study: STM observation on a cantilever sample that detects sample bending. Graph (a) illustrates evolutions of deflections at the free end of the cantilever samples during Br_2 exposure to clean Si(111)−7×7 surfaces at room temperature. Negative capacitance values imply that the surface is expanded from the initial condition, while positive values correspond to surface shrinkage. This illustrates compressive and tensile stress conditions, respectively. The red curve and the blue-green curve correspond to two different exposures under the same conditions. Images (b)–(d) were taken at the position indicated on the curves by the arrows. The image sizes of (b), (c), and (d) are 11.2×8.9, 14.7×14.2, and 30.0×22.1 nm^2, respectively.

This thermal drift effect diminishes greatly over time, particularly after the sample has been prepared by flashing. Comparing our value for the thermal drift with the value of -2.8×10^{-7} pF/s estimated from a previous report,[19] we see that our thermal drift effect is 86% smaller. Our thermal stability may be attributed to the good choice of materials for our sample holder setup. This result is important since small thermal drift is essential for a reliable long time measurement. In addition, we can estimate the electrical stability by subtracting the thermal drift effect. As a result, the average capacitance value and the variance were calculated as $\mu=2.517\,990\,1$ pF and $\sigma_\nu=1.9\times10^{-6}$ pF, respectively. Statistically speaking, $\pm\sigma_\nu$ around μ corresponds to an accidental error. Although this is slightly inferior to the ideal detection limit of $(0.5-0.8)\times10^{-6}$ pF, it has an almost ideal resolution. Consequently, while strictly keeping the environment thermally and electrically quiet, we have the capability to perform stable capacitance measurements.

Preliminary results of a simultaneous study

Here, we demonstrate an example of a simultaneous study to observe atomic structures via STM on a cantilever sample that is detecting sample bending. Figure 9(a) displays two evolutions of the displacement of the cantilever sample during Br_2 exposure to the Si(111)-7×7 surface at room temperature. Both evolutions were taken with equivalent current conditions through the halogen pellet source, namely, 25.7 μA. In this experiment, the Br_2 species were created with the use of an electrochemical cell.[28] This consists of a halogen pellet composed of AgBr, a filament for pellet heating, a base plate below the pellet and a nozzle [1/8 in. diameter stainless pipe shown in Fig. 6(a)]. In the pellet, negative ions, i.e., Br^-, diffuse according to the electric field. At

Downloaded 26 Sep 2007 to 133.48.150.181. Redistribution subject to AIP license or copyright, see http://rsi.aip.org/rsi/copyright.jsp

the top surface of the pellet, the Br_2 species can be successfully created and are exposed to the Si(111)-7×7 surface via a nozzle.

In Fig. 9(a), it is evident that both evolutions display similar signatures. Small differences exist, however, which may be caused by a simple geometrical error.[19] Initially, steep surface expansion occurred, followed by slight surface relaxation. In the case of the red curve, the maximum expansion was −4.7 N/m, while the blue-green series exhibited a lower expansion, i.e., −2.97 N/m. Following this maximum expansion, a slight relaxation was observed (0.64 N/m for the red curve and 0.41 N/m for the blue-green series). From the red curve it is clear that following this relaxation feature, no other major attributes are evident; the curve saturates to a constant value.

Intrinsically, a clean Si(111)-7×7 surface is under a tensile surface stress condition.[29] Adatom structures are major contributors to this tensile state. This surface can be easily modified via reaction with Br_2. Initially, dangling bonds of adatoms, rest atoms, and corner holes are plausible candidates for reaction with bromine species. In a single unit cell, there are 12 adatom dangling bonds, 6 rest atom dangling bonds, and 1 corner hole dangling bond. Even if the probabilities of reacting each dangling bond site are the same, the effect from adatom sites should be dominant due to their majority. This should induce a reduction of the intrinsic tensile stress condition. After some time, the adatom backbonds may react, which, in turn, may induce desorption of these structures. In addition, steric effects and electrostatic repulsions between adsorbed Br atoms may occur due to their large size and large electronegativity. This may also induce surface expansion. For these reasons, any explanation of observed surface expansion is highly speculative at this stage. On the other hand, the feature representing slight stress relaxation may have been caused by the back side reaction of the cantilever sample. Although the effect from the front side of the sample is dominant (due to the configuration of our system), it is difficult to suppress the back side effect completely.

Figures 9(b)–9(d) are useful in developing our interpretation of the reaction progress. Figure 9(b) displays a noticeable depression in the number of ad-atom sites. In addition, a small number of single features, which are brighter than the original adatom structures, are also visible. In Fig. 9(c), the numbers of reacted adatom sites and bright single features have increased. Finally, in Fig. 9(d), most adatom sites have vanished while a number of bright single features remain. At this stage, the majority of dangling bond sites has reacted. However, the existence of bright single features was not expected from the stress evolution. These bright features may represent intermediate states of the reaction process. A more detailed STM study is required to explain the entire behavior of the stress evolution. Here, we have provided only a brief explanation of events during Br_2 exposure to Si(111)-7×7 at room temperature, as the main purpose of this article is to introduce the system which we have developed. More detailed reports into the various reactions studied using this system will be discussed elsewhere.

Recently, we have obtained an additional successful result relating to the initial oxidation of Si(111)-7×7 surfaces. The stress signature displayed two compressive stages during the initial oxidation process. STM observation on the same cantilever sample evidently elucidated the origin of the stress evolution to be "unit selective oxidation of the faulted half units."[30] This result also confirms the benefit of our newly developed system.

SUMMARY

In this article, we have introduced a system to study the underlying origins of forces on solid state surfaces from the viewpoint of atomic surface morphology. To measure surface forces, a large cantilever sample together with a capacitive detection method was used. A STM was incorporated to observe atomic structures on the cantilever surface. Using a large cantilever sample provides us with flexibility to choose a range of cantilever materials with various surface orientations. To achieve good thermal stability, a combination of low thermal expansion materials was used for the sample holder, super invar, and quartz. This choice of materials showed minuscule thermal drift. This is essential for reliable force and structural measurements. STM measurements are not trivial due to the natural oscillation of the cantilever sample. To overcome this problem, an appropriate choice of sample dimensions is essential.

Prior to this article, a similar simultaneous study was reported.[18] In their study a STM was used not only to observe atomic structures, but also to detect the displacement of the Au cantilever sample. As mentioned in their report, the noise levels are larger than those for conventional STM. As a result, individual atoms were not distinguishable. They attributed this problem solely to poor sample rigidity on mounting. However, to observe such small corrugations on the metallic reconstructed surface, it is essential to address the self-oscillation issue. In addition, the STM method fails to provide a measure of absolute sample displacements. In our case, the capacitance method allows for absolute determination of sample displacements and also provides us with a superior deflection resolution. As shown in this article, the resolution we achieve is adequate to study the origins of forces in atomic scale structures and phenomena on surfaces. Using our system, we have the capability of investigating a wide range of surface processes.

ACKNOWLEDGMENTS

The authors would like to thank T. Uchihashi, T. Fukuma, K. Miki, I. Shiraki, and M. Kitajima for helpful technical advice and discussions. They would also like to thank Y. Niino, N. Ohtani, and T. Endo for their constant support in building this system. This project was carried out with the support of the Science Foundation Ireland (SFI) under Grant No. 00/PI.1/C077 and the Centre for Research on Adaptive Nanostructures and Nanodevices (CRANN).

[1] R. P. Feynman, Phys. Rev. **56**, 340 (1939).
[2] J. J. Boland, J. Vac. Sci. Technol. B **9**, 764 (1991).
[3] J. J. Boland, Surf. Sci. **261**, 17 (1992).
[4] J. J. Boland, Science **256**, 1304 (1992).
[5] R. Koch, D. Winau, and K. H. Rieder, Phys. Scr., T **49**, 539 (1993).

Downloaded 26 Sep 2007 to 133.48.150.181. Redistribution subject to AIP license or copyright, see http://rsi.aip.org/rsi/copyright.jsp

[6] A. J. Schell-Sorokin and R. M. Tromp, Phys. Rev. Lett. **64**, 1039 (1990).
[7] C. F. Herrmann, D. Chen, and J. J. Boland, Phys. Rev. Lett. **89**, 096102 (2002).
[8] M. Fouchier and J. J. Boland, Phys. Rev. B **57**, 8997 (1998).
[9] H. Ibach, Surf. Sci. Rep. **29**, 193 (1997).
[10] R. Koch, D. Winau, and K. H. Rieder, Phys. Scr. **49**, 539 (1993).
[11] A. Kurokawa, T. Narushima, K. Nakamura, H. Nonaka, S. Ichimura, A. N. Itakura, and M. Kitajima, Jpn. J. Appl. Phys., Part 1 **43**, 281 (2004).
[12] T. Narushima, T. Kurashina, A. N. Itakura, T. Kawabe, and M. Kitajima, Appl. Surf. Sci. **159–160**, 25 (2000).
[13] T. Narushima, A. N. Itakura, T. Kawabe, and M. Kitajima, Appl. Phys. Lett. **79**, 605 (2001).
[14] T. Narushima, M. Kitajima, and K. Miki, J. Phys.: Condens. Matter **16**, L193 (2004).
[15] T. Narushima, N. T. Kinahan, and J. J. Boland, Rev. Sci. Instrum. **76**, 095113 (2005).
[16] T. Fukuma, M. Kimura, K. Kobayashi, K. Matsushige, and H. Yamada, Rev. Sci. Instrum. **76**, 053704 (2005).
[17] M. Helm, J. J. Servant, F. Saurenbach, and R. Berger, Appl. Phys. Lett. **87**, 064101 (2005).
[18] C. E. Bach, M. Giesen, H. Ibach, and T. L. Einstein, Phys. Rev. Lett. **78**, 4225 (1997); H. Ibach, C. E. Bach, M. Giesen, and A. Grossmann, Surf. Sci. **375**, 107 (1997).
[19] D. Sander and H. Ibach, Phys. Rev. B **43**, 4263 (1991).
[20] T. R. Albrecht, P. Grütter, D. Horne, and D. Rugar, J. Appl. Phys. **69**, 668 (1991).
[21] Omicron NanoTechnology GmbH, Limburger Str. 75, 65232 Taunusstein, Germany.
[22] G. Gerald Stoney, Proc. R. Soc. London, Ser. A **82**, 172 (1909).
[23] R. W. Hoffman, *Mechanical Properties of Non-Metallic Thin Films: In Physics of Non-Metallic Thin Films*, Proceedings NATO Advanced Studies Institute, Series B: Physics, edited by C. H. S. Dupuy and A. Cachard (Plenum, New York, 1976), Vol. 14, pp. 273–353.
[24] Model AH 2550A, Ahandeen-Hagerling, Inc., 31200 Bainbridge Road, Cleveland, OH 44139-2231 (http://www.andeen-hagerling.com/ah2550a.htm).
[25] W. A. Brantley, J. Appl. Phys. **44**, 534 (1973).
[26] J. T. Yates, Jr., *Experimental Innovations in Surface Science* (Springer, New York, 1998).
[27] Model GVH398 (modified), Thermo-RIKOH, Thermo RIKO Co., Ltd., Mitaka High-Tech Center, 8-7-3 Shimorenjaku, Mitaka City, Tokyo 181-0013, Japan. (http://www.kagaku.com/thermo/).
[28] N. D. Spencer, P. J. Goddard, P. W. Davies, M. Kitson, and R. M. Lambert, J. Vac. Sci. Technol. A **1**, 1554 (1983).
[29] D. Vanderbilt, Phys. Rev. Lett. **59**, 1456 (1987).
[30] T. Narushima, N. T. Kinahan, J. J. Boland, and K. Miki (unpublished).

Downloaded 26 Sep 2007 to 133.48.150.181. Redistribution subject to AIP license or copyright, see http://rsi.aip.org/rsi/copyright.jsp